



Water-Borne Erosion Estimation Using the Revised Universal Soil Loss Equation (RUSLE) Model Over a Semiarid Watershed: Case Study of Meskiana Catchment, Algerian-Tunisian Border

Anissa Mahleb · Riheb Hadji  · Farid Zahri · Rania Boudjellal · Abdelmohcen Chibani · Younes Hamed

Received: 9 October 2021 / Accepted: 22 April 2022 / Published online: 16 May 2022
© The Author(s), under exclusive licence to Springer Nature Switzerland AG 2022

Abstract Soil erosion is one of the major environmental problems in the Middle East and North Africa (MENA) region. Favoured by the harmful effects of climate change, and intensified by heavy rainstorms, droughts, runoff, soil features, and land cover; the Meskiana catchment, NE Algeria suffers hugely from this hazard. The main purpose of the present study is to adapt the RUSLE model to map the spatial distribution of soil erosion susceptibility in dry climate watershed based on the geographic information system (GIS) and remote sensing (RS) technique. The model considers erosivity (R), topography (LS), erodibility (K), cover management (C), and support practice (P) as the main predisposing and triggering parameters of the phenomenon. For data processing,

slopes, precipitations, lithofacies, Normalized Difference Vegetation Index (NDVI), drainage density, and land use were integrated. Some parameters of the model were estimated using RS data and the erosion susceptibility was mapped using GIS. The results showed that the annual soil loss is about 61 t/ha/year in the entire study area, and identified the most heavily eroded areas, requiring immediate action. The compilation of GIS-RS geospatial technologies with field survey made it possible to assess the spatial variation of soil erosion quantitatively and rapidly. It can assist managers in the implementation of land degradation mitigation program with low-costs and enhanced accuracies.

A. Mahleb · R. Hadji (✉) · F. Zahri · A. Chibani
Department of Earth Sciences, Institute of Architecture and Earth Sciences, University of Ferhat Abbas, Setif, Algeria
e-mail: hadjirihab@yahoo.fr

A. Mahleb · A. Chibani
Emerging Materials Research Unit, University of Ferhat Abbas, Setif, Algeria

R. Hadji · F. Zahri
Laboratory of Applied Research in Engineering Geology, Geotechnics, Water Sciences, and Environment, Setif 1 University, Setif, Algeria

R. Hadji · F. Zahri · Y. Hamed
International Association of Water Resources in the Southern Mediterranean Basin, Gafsa, Tunisia

R. Boudjellal
Water and Environment Laboratory, Department of Earth Sciences and Universe, Larbi Tebessi Tebessa University, Tebessa, Algeria

Y. Hamed
Faculty of Sciences of Gafsa, University of Gafsa, Gafsa, Tunisia

Y. Hamed
Laboratory for the Application of Materials to the Environment, Water and Energy (LAMEEE), City Campus Sidi Ahmed Zarroug, 2112 Gafsa, Tunisia

Keywords Land degradation · Rainfall · Topography · Erodibility · Land cover

1 Introduction

Natural hazards threaten permanently the people throughout the world. The quantization of brutal events such as earthquakes, mass wasting, and floods requires the estimation of the hazard/susceptibility level of the specific risk and the consideration of the vulnerability degrees, (Hadji et al. 2013, 2014a 2016, 2017; Mekki et al. 2017; Dahoua et al. 2017a, b, 2018; Manchar et al. 2018; Zeqiri et al. 2019; Anis et al. 2019; Fredj et al. 2020). However, for long-term perils, such as shrinkage-swelling and soil erosion, the concept is quite different (Hadji et al. 2014b). The environmental issues related to water have been dealt with in countless works, dealing with a lot of aspects (Rouabhia et al. 2012; Hamed et al.

2014, 2021; Mokadem et al. 2016; Besser et al. 2018, 2021; Ncibi et al. 2020a, b, 2021; Benmarce et al. 2021; Bensoltane et al. 2021; Hamad et al. 2021a, b).

Water-borne erosion is the worst form of land degradation in the MENA countries. It causes severe socio-economic and environmental problems (Fig. 1), and leads to soil loss, water-quality degradation, and dam siltation. The rate of soil erosion is controlled by different parameters of the basin such as geology, geomorphology, climate as well as hydrological dynamics. Global projects as the United Nations Environment Program (UNEP) or the United Nation Convention Desertification Combat (UNCDC) have dealt with this problem. According to the Global Assessment of Human-induced Soil Degradation project (GLASOD), about 15% of the land surface has already degraded (Oldeman et al. 1991). The hardest rates of soil erosion were reported in Europe (25%), Asia (18%), Africa (16%); and less in North America (5%). Algeria is one of most affected



Fig. 1 Photos of some disasters caused by the effect of water erosion

countries by the phenomenon in North Africa (Hamed et al. 2018), the western part is particularly eroded, with 47% of losses in fertile lands; followed by the middle (27%) then the East (26%). The specific erosion reaches 4000 t/ km² year, and the siltation rate exceed 15% (Bougerra et al. 2017).

The evaluation models of soil erosion make available the quantification of the process under various conditions (Aiello et al. 2015). By consulting the geoscientific literature; we noticed different studies that rigorously discussed the spatio-temporal interactions between soil erosion and controlling factors. They vary from empirical, physical to conceptual models (Viney and Sivalapan 1999). Empirical-based models are the simplest and the widely applied (Merritt et al. 2003). The Universal Soil Loss Equation (USLE) method was initially developed by Wischmeier and Smith (1965), Modified (MUSLE) by Williams and Berndt in (1977), then Revised (RUSLE) by Renard (1997). The latest RUSLE version has proven a great ability to estimate the soil loss (Alexakis, et al. 2013; Xiao et al. 2015).

Because of their high cost, long time-consuming and large study areas; the conventional methods to assess water-born erosion no longer fit with the current natural hazard mapping needs. The advent of RS data and the GIS environments gave the necessary support to these methods (Ganasri and Ramesh 2016; Nezhadafzali et al. 2019; Mohammed et al. 2020). The RS/GIS geospatial algorithms allow the prediction of the erosion potential in large expanses on a cell-by-cell basis (Tamene et al. 2017; Thapa, 2020). They have the ability to integrate complex factors such as soil, climate, vegetation, terrain, and human practice (Teng et al. 2018). The Meskiana catchment is characterized by an acute orography, a semi-arid climate, rainfall-stormy precipitation, torrential/intermittent runoff and silty-clay surface soil textures. These factors favoured the intense susceptibility to erosion. We have chosen to apply RUSLE model in our study because the method proved in many close contexts to be a simple and practical in the investigation of the soil erosion process.

The main purpose of the present article consists in the implementation of an environmental info-system based on the RUSLE model that considers all the causative factors of water-born erosion to assess of the soil-loss susceptibility in the Meskiana catchment. The method passes through: (i) The geo-processing of soil

loss controlling parameters in the study area; (ii) The implementation of an approach that combines RS data and GIS to estimate the spatial distribution of water born-erosion and soil loss through RUSLE model; (iii) The study of geochemical and mineralogical terrain features; and (iv) the identification of the most affected area.

The outcomes of the study could help in the establishment of effective management scenarios and provide skills to decision-makers for mitigate the soil erosion threats.

2 General Settings

The Meskiana catchment is a large watershed situated between the 07°11' 48" to 07° 54' 12" longitude, 35° 09' 35" to 35° 48' 06" latitude and covers about 1680 km² of land near the Algerian-Tunisian international border (Fig. 2a), (Tamani et al. 2019). The study region have an semi-arid climate characterized by a hot dry summer and a temperate cold winter with an average annual rainfall of 400 mm and a temperature of 16.3 °C (Hamad et al. 2021a, b). The average annual evaporation fluctuates between 1300 and 1500 mm (Rais et al. 2017; Hamad et al. 2018a, b). The land use of the catchment shows barren lands, cereals, rangelands forests, and olive groves. The Halfa steppes are scarce in the basin, indicating poor protection against water erosion. The morphology of the basin is characterized by hills alternating with valleys and steep mountains (Boulema et al. 2021). Geologically, the formations are made up of Triassic facies, emerging in diapirs; Cretaceous stacking of Aptian and Maastrichtian age formed by marl and limestone, and of Miocene sandstone limestone formation; covered in the middle of the basin by a Mio-Plio-Quaternary continental filling (Mouici et al. 2017). The outcrops represent 56% of marl, 26.5% of alluvium, 3% of limestone, and 3% of Triassic (Fig. 2b, c) (Nekkoub et al. 2020; Brahmi et al. 2021). The soil of the watershed exhibits a swelling character with sensitivity to erosion (Table 1). This soil is a clay loam (Table 2). The diffractometric analysis and fluorescence spectra of clay minerals identify the types of clay minerals in samples collected from the main outcrops of the study area (Fig. 3). The fluorescence showed a consequent rate of Alumina. This geochemical class favors the development of the

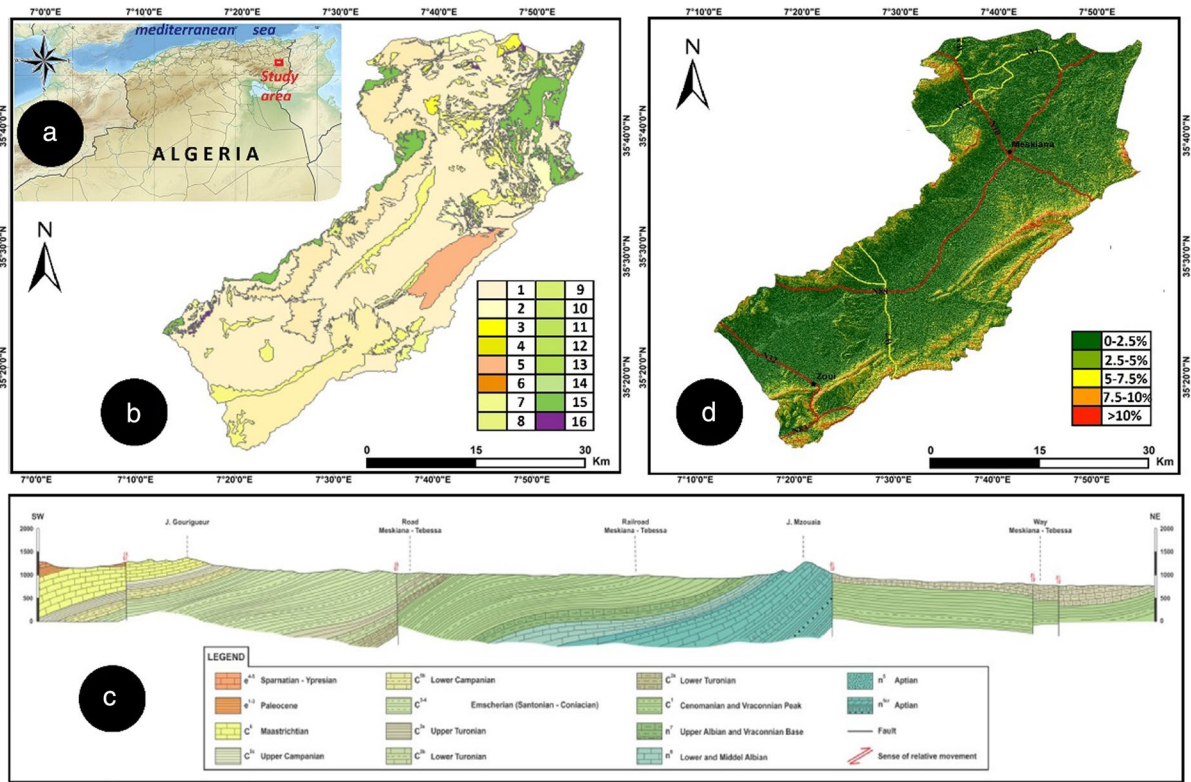


Fig. 2 a Geographic location of the study area, b Simplified lithofacies map of the study area; c geologic cross-section in Meskiana catchment, d=slope map of the study area. [Legend of b: 1: Quaternary, 2: Plio-quaternary, 3: Middle Miocene;

4: Lower Miocene, 5: Ypresian and Lutecian, 6: Thanetian, 7: Upper Maestrichtian, 8: Campanian, 9: Santonian, 10: Coniacian, 11: Upper Turonian, 12: Lower Turonian, 13: Upper Cenomanian, 14: Aptian, 15: Cretaceous, 16: Triassic

Table 1 Argillosity and organic matter content of the analysed soil samples

No	Vbs (NF p94-068)	OM (NF p 94-055)	Caco ₃ (NF p 94-048)
1	1.33	2.65	52
2	2.83	1.86	21
3	3.66	1.34	41
4	6.16	1.28	33

Table 2 Soil goniometric size (LCPC standards)

Sample	01	02	03	04
%Gravel (2 < Φmm < 60)	03%	04%	01%	03%
% Sand (0.06 < Φmm < 2)	16%	14%	10%	12%
% Silt (0.002 < Φmm < 0.06)	68%	73%	65%	70%
% Clay (Φmm < 0.002)	13%	09%	14%	11%

phenomenon at the microscopic scale (Table 3). The fluctuation of the piezometric level depends closely on the contributions of precipitation (Demdoum et al. 2015). The watershed is drained by the wadi Meskiana; the main collector of runoff water. On the right bank, spills wadi Rbâa, wadi Hmadjra, wadi Smar el Houd and Wadi El Mallah. Whereas, on the left bank, spills wadi Jdida and wadi Ain Sedjra. The study area shows a hilly terrain with high to moderate slope ranging from 49.56% in the mountains ridges to sub-flat in the river basins, (Fig. 2d).

3 Materials and Methods

In order to rank the most susceptible areas to soil erosion, various thematic layers were rasterized and integrated into GIS software. The modelling

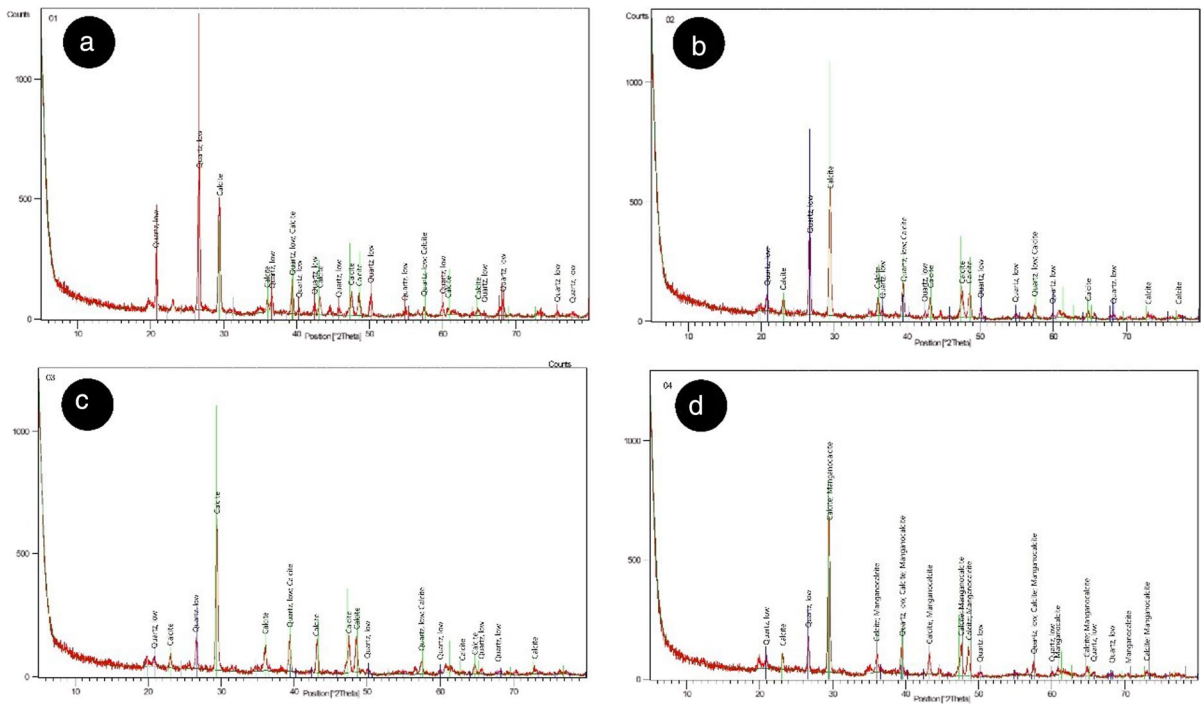


Fig. 3 XRD of the samples from the main outcrops of the study area

involved a weighted overlay of the five factor maps. The higher weight is given to the feature with the highest influential factor and the lower to the least influential one. The RUSLE model combines five factors: rainfall (R), topography (LS), soil erodibility (K), cover management (C), and support practice (P) (Wischmeier and Smith 1978). The model can be mathematically expressed by the Eq. (1)

$$A = R * K * LS * C * P \tag{1}$$

where **A** is the annual rate of soil loss (t/ha/yr); **R** is the rainfall erosivity ($MJ\ mm^*m^{-2}\ h^{-1}$); **K** is the soil erodibility factor ($t*ha\ J^{-1}*mm^{-1}$); **LS** are slope length and slope steepness factor (dimensionless); **C** is the cover and management factor (dimensionless in %); **P** is the support practice factor (dimensionless in %).

The flow chart of the present study can be used as a practical method for the estimation of the soil loss (Fig. 4).

3.1 Data Used

The study area watershed has been bounded in ArcGIS 10.3 software under the hydrology/spatial analyst tools. The prepared base map was then used for the extraction of study area from the satellite image and Shuttle Radar Topography Mission digital elevation model (SRTM-DEM). For remote sensing; we used Sentinel 2-A satellite data earned on January 1st 2018 for generating all the needed maps layers. The designation of the geology has relied on the Oum El Bouaghi, Ain Beida, El Aouinet,

Table 3 Results of XRF

N°	Chemical composition	Sample 01	Sample 02	Sample 03	Sample 04
1	Na ₂ o	0.317	0.159	0.318	0.197
2	Mgo	2.51	1.69	1.71	1.82
3	Al ₂ O ₃	12.2	13.2	11.4	12.2
4	Sio ₂	44.5	34	30.1	36.1
5	P ₂ O ₅	0.299	0.176	0.207	0.21
6	So ₃	0.656	0.255	1.66	0.742
7	Cl	0.0585	0	0	0.0166
8	K ₂ O	1.84	1.09	1.08	1.22
9	CaO	31.4	41.9	46.4	36.3
10	TiO ₂	0.663	0.894	0.849	1.03
11	Cr ₂ O ₃	0.0212	0	0	0.0495
12	MnO	0.0609	0.0489	0.0449	0.0389
13	Fe ₂ O ₃	5.33	6.61	5.97	7.39
14	NiO	0.0129	0.0108	0	0
15	ZnO	0.00119	0.0110	0	0
16	Br	0.0052	0	0	0
17	Rb ₂ O	0.0111	0.0042	0.0063	0.0067
18	SrO	0.100	0.190	0.194	0.163
19	Y ₂ O ₃	0.0030	0	0	0
20	ZrO ₂	0.0299	0.0195	0.0127	0.0197
21	Nb ₂ O ₅	0.0023	0	0	0
22	ReO ₂	0	0	0.0326	0

Graet El Tarf, Fkirina, Meskiana, Khenchela, Dalâa, Hammamet, Jebel Djehfa, and Zoui 1:50,000 scale, geologic maps in the same GIS environment. Twelve weather stations located at the within the study area or in its vicinity, and rainfall data for 20 years (2000–2020) was collected from the (ONM National Meteorological office) database. Extensive

field survey data and field images were used for calibration, processing, and result validation.

3.2 Predictive Factors

3.2.1 Erosivity

Estimating the erosivity factor "R" according to the Wischmeier and Smith (1978) formula requires knowledge of the kinetic energies (ec) and the 30-min average intensity (*i*₃₀) of the raindrops in each down-pour. "R" is given by the Eq. (2)

$$R = k.ec.i_{30} \tag{2}$$

With "k" is a coefficient depending on the system of measurement units.

However, the precipitation data available in the stations of our study area are only monthly or inter-annual averages.

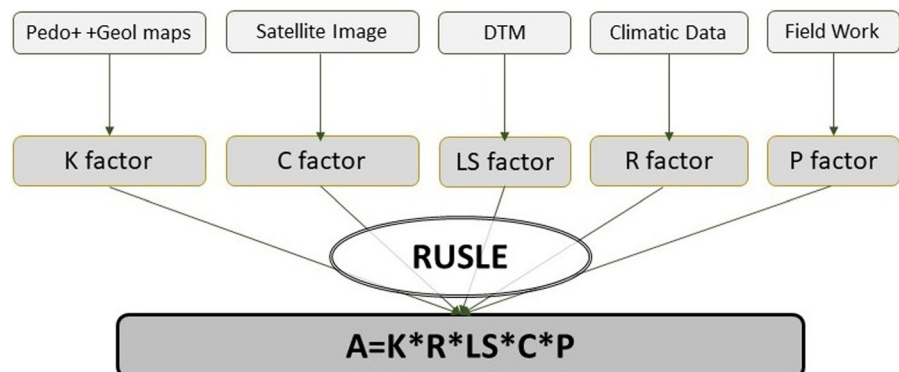
Authors such as Arnoldus (1980) have developed alternative formulas that involve monthly and annual precipitation to determine "R" factor. The formula of Rango and Arnoldus (1987) was already successfully applied to twelve sites in the greater Maghreb; hence the formula corresponds well to our study area (Eq. 3):

$$\log R = 1.74.\log \sum \left(\frac{P_i^2}{P} \right) + 1.29$$

With: "R" rainfall erosivity factor expressed in t/ha.

Where *P_i* is monthly precipitation and *P* is annual precipitation in mm; calculated using a large number of rainfall stations, subsequently the results were interpolated over the rest of the basin. The calculation of the erosivity factor r is applied over a series of

Fig. 4 The adopted methodological Flow chart for soil erosion assessment



twenty (20) years of precipitation in and around the watershed.

3.2.2 Erodibility

The adjustment of "K" factor for coarse elements was based on the soil map of the Meskiana watershed; several samples were analysed to identify the characteristics of each type of soil. Thus, the relation was used for the estimation of this factor calculated by the Nomogram equation, which makes a combination between the size of the particles, % of the organic matter, the structure of the soil and the class of the permeability of the profile according to the Eq. (4):

$$K = [(2.1(10^{-4})m + 1.14(12 - om)) + ((3.25(s - 2)) + (2.5(p - 3)))] / 100 \tag{4}$$

with: K: soil erodibility determined on an annual basis expressed in t.h/ha. Mj.mm; om: organic matter content in %; m: textural term = (silt + fine sand) % * (100—clay%); s: soil structure code (1 to 4), 1 for a very fine grained structure and 4 for a massive structure; p: permeability code (1 to 6), ranging from 1 for fast-draining soils to 6 for very slow-draining soils.

The erodability class is ranked as low when K is between 0.1 and 0.2; as moderate if K is from 0.2 to 0.30 and as high if K is between 0.30 and 0.40.

3.2.3 Topography

"LS" is a topographic factor combining the slope (*s* in %) and the slope length (*l* in m) (Wischmeier and Smith 1965). LS is calculated from the slope inclination and slope length, obtained from the geo-processing of DEM in GIS software using Moore and Burch's formula (Eq. 5):

$$LS = 1.6 * pow([flowacc] * resolution / 22.1, 0.6) * pow(\sin([\text{slope}] * 0.01745) / 0.09, 1.3) \tag{5}$$

The classes of LS factor are ranked as follows: If slope = [0, 7.0%] so LS = 0.55. If *s* = [7, 11.3] so LS = 0.6, If *s* = [11.3, 17.6] so LS = 0.8; If *s* = [17.6, 26.8] so LS = 0.95 and if *s* is > 26.8 so LS = 1.

3.2.4 Cover Management

RS algorithms have the ability to generate the land use-land cover of the study area. "C" factor represents the effect of vegetation cover. Based on the normalized vegetation index NDVI derived from Sentinel 2 A imagery. The index transforms the reflectance of vegetation into a percentage (Karaburun 2010). The relationship between the NDVI and the "C" parameter is determined by the Eq. (6), (Benselama et al. 2018)

$$C = 0.9167 - NDVI * 1.1667 \tag{6}$$

3.2.5 Support Practice

The factor "P" integrates anti-erosion cultivation techniques, such as contour crops, alternating strips or terraces, reforestation in benches, and ridging. The values of the anti-erosion practice factor of human origin are extracted according to the sloping cultivation methods cited by (shin, 1999). According to Gitas et al. (2009), the P factor is calculated as the ratio of the rate and amount of soil loss due to a specific support practice to the soil loss due to row farming in upward and downward of the slope condition. The "P" values ranges between 0 and 1, in which the highest value is given to the areas where there is absence of any conservation practices such as grasslands and open areas, and the minimum values are assigned to plantation area with contour cropping and built-up land.

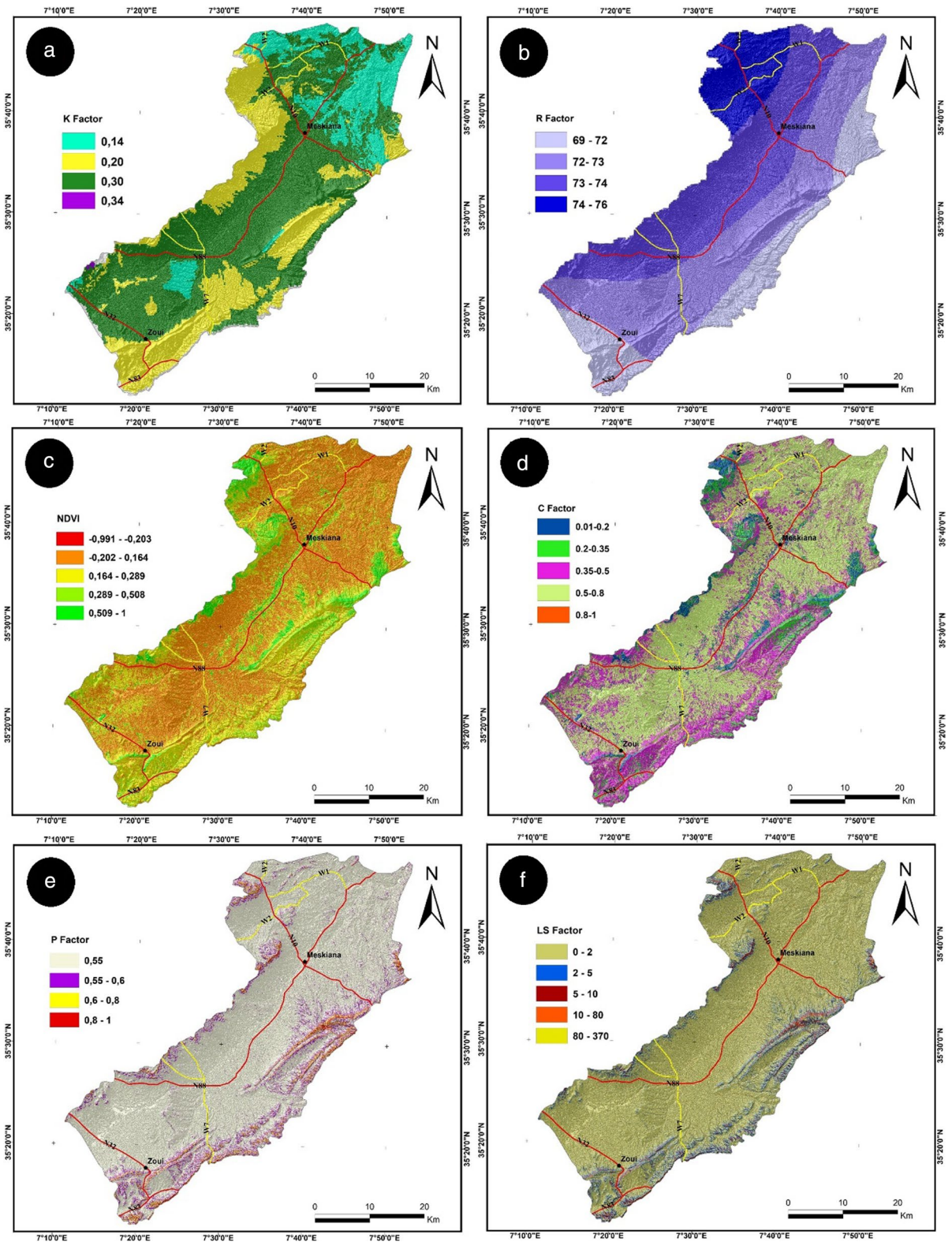


Fig. 5 Spatial repartition of: **a**=K Factor, **b**=R factor, **c**=NDVI, **d**=C factor, **e**=P factor and **f**=LS factor

4 Results and Discussions

4.1 Parameter Estimation

4.1.1 Assessment of Soil Erodibility

The erodibility of soils represents the susceptibility of soil to erosion reflected by the rate of soil loss under a standard rainfall condition estimated on the basis of soil textures (Cassol et al. 2018). Nomograph is used to determine the "K" factor for a soil, based on texture (m); % organic matter (om), soil structure (s), and permeability (p) according to Wischmeier and Smith (1978) model; who incorporates a corrective factor to take into account coarse diameters. The model is well suited to the soil nature of arid and semi-arid environments in the MENA region." K" factor is determined according to the Eq. (4):

The calculated values of the erodibility index "K" vary between 0.14 and 0.34 (Fig. 5a). They are divided into four classes of soils. The calculated "K" erodibility values for each type of soil show that almost all the soils (93.6%) have moderate erodibility (0.20–0.30). Vertisols have low erodibility (0.10–0.20), they are the least represented in the region (2%). Some poorly evolved soil exhibits high erodibility rates (0.30–0.40), occupying 3.9% in the Southwest of the study area. The comparison of the pedological map with the topography shows that the little developed soils on steep slopes, bordering the valleys where soil degradation is very intense.

4.1.2 Assessment of Rain Erosivity

The rainfall erosivity was calculated according to the modified Fournier equation (Arnoldus 1980) using the monthly rainfall of agricultural years, (September to August), over the period 2000–2020, from 12 pluviometric stations located at the within the study area and in its vicinity. We noted that the used rainfall series corresponds to a relatively dry period. The average value of the rainfall erosivity over 2000/2020 period was obtained by performing the monthly and annual average precipitation calculated for each year. The distribution of the different classes of rainfall erosivity "R" in our study basin is shown in Fig. 5b.

4.1.3 Vegetation Cover and Cultural Practices Factor

The "C" factor combines vegetation cover, the degree of plant production, and the associated cultivation technique. The factor varies between 1 for bare soil to 0.1 for dense forests. The spatial distribution of vegetation covers and cultural practices shows that areas most vulnerable to erosion are the "bare land" land-use type. This class covers almost the entire upstream of the catchment (Fig. 5c). According to the "C" factor map (Fig. 5d); the study area has been classified into five major soil classes; the lowest value (0.0007) is on land planted with agriculture and arboriculture, however, the coefficients of 0.8 to 0.9 are found in areas covered by sparsely dense and spaced forests. The highest coefficients (close to 1) correspond to bare land.

4.1.4 Anti-Erosion Practice

The "P" factor determines the ratio of soil loss to specific practices on agricultural land, especially with parallel plowing against slopes (Wischmeier and Smith 1978). Note that in our study the low and medium values of "P" are assigned to areas with low to moderate slopes. The factor varies from 0.55 to 0.6 for areas with a low slope, and from 0.8 to 1 for areas with steep slopes (Fig. 5e).

4.1.5 Topographic Factor (LS)

The length and inclination of the slope influence the erosion process. We used a 30 m SRTM DEM for the slope, exposure, slope length, and LS calculation in Arcgis 10.3 software. The stretched values of the LS were grouped into five classes. 60% of the catchment area belongs to very high areas (Fig. 5f). It is concentrated in the upper valley and in intrusive areas of the Wadi Meskiana tributaries in the southern part of the basin. The lowest values of the LS index (which vary from 0 to 5) occupy only 7% of the surface of the basin.

4.2 Estimation of the Erosion Rate

An erosion rate of soil loss results from the combination of the the erosivity of precipitation, the erodibility of soils, the combined effect of the degree and

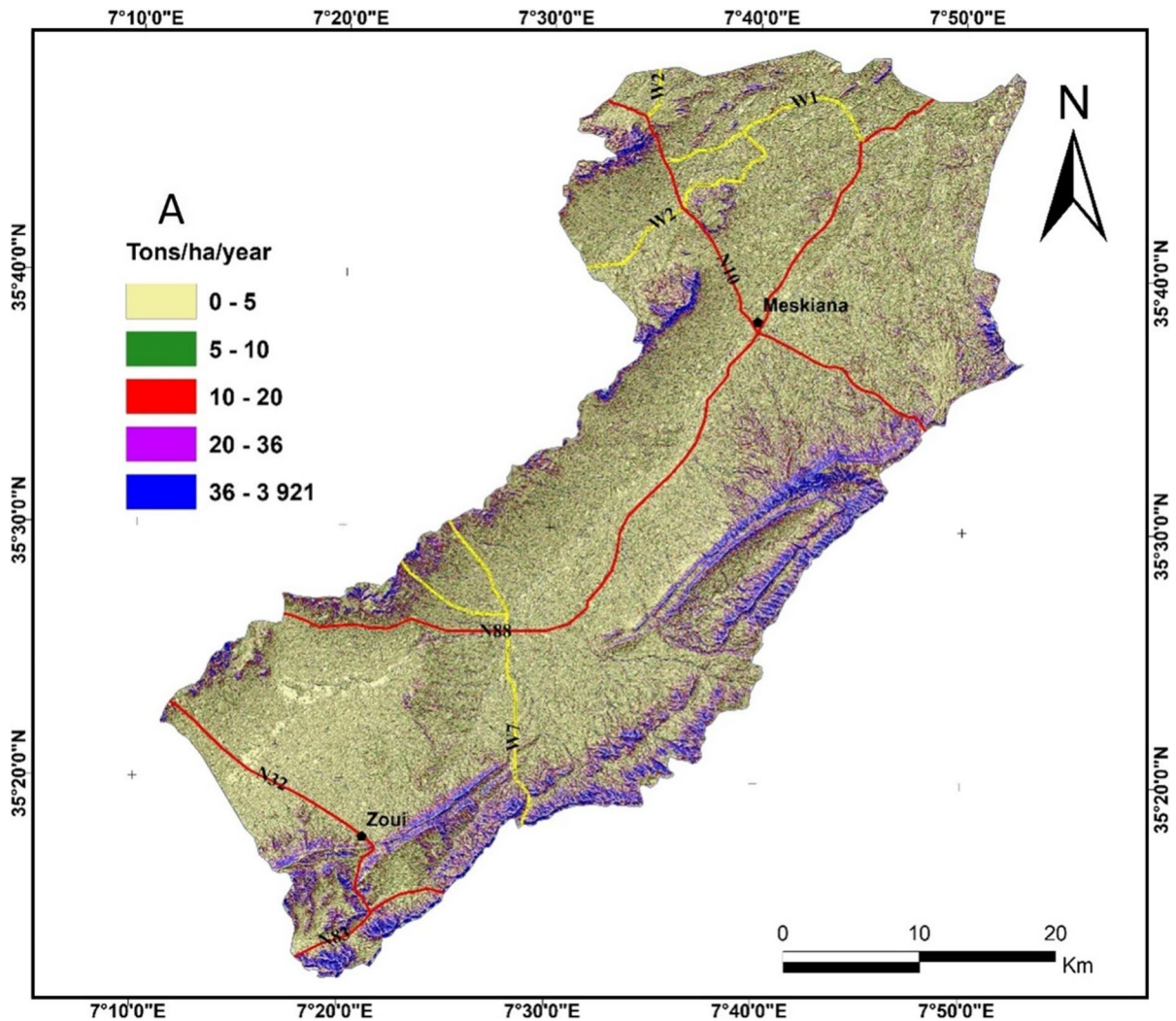


Fig. 6 The spatial distribution of the potential of erosion in the study area

the length of the slope, the vegetation cover, and anti-erosion practices in the RUSLE model. The five factor maps were multiplied with Raster Calculator/Map Algebra tools, to calculate the annual rate of soil loss (t/ha/yr); in the study area on a pixel-by-pixel basis scale (Fig. 6).

The weighted average loss per unit area is 61 t/ha/year or a total of 742,674 t/year for the entire basin. The losses vary between 34.65 t/ha/year as the minimum value measured in the matorrals and 129.12 t/ha/year as the maximum value estimated at the level of the rangelands. Average losses are estimated in the plain at 46.5 t/ha/year on the most resistant soils where the forest cover is fairly dense. The land

cultivated by seasonal crops and arboriculture shows high susceptibility to erosion with annual losses of 57.61 t/ha and 64.36 t/ha/year respectively. The map of average annual soil losses shows a clear fragility of the eastern and north-eastern part of the basin on marl and Miocene sandstone marls where values exceed 35 t/ha/year. These cover approximately 3250 ha or 27% of the total area of the catchment. The weak losses (< 7 t/ha/year) dominate the slopes of the right bank of the basin where a scrub of holm oak and reforestation cover the sandstone grounds.

Several studies have proved the improvements made by the adoption of the GIS-RS technology to the RUSLE method. Perhaps the most important is

the estimation and mapping of "R" factor into a raster surface using the IDW Interpolation technique (Panditharathne et al. 2019). In addition, the combination of GIS/RS enabled the derivation of "LS" factor with better accuracy at the large catchment scale, and in complex landscapes (Wilson and Gallant 2000). Without the use of GIS-RS, obviously, the results will be less precise with low spatial resolution. Although, we recommend the approval of RUSLE based GIS/RS model as an effective tool for soil erosion hazard mapping at the catchment scale. The main limitation of the technique implicate the inability to validate the model with accurate tools such as (Area Under Curve (AUC) of the receiver operating characteristic (ROC) curve) and the deficiency to compare between the calculated and the standardized soil loss values (Somasiiri et al. 2021).

5 Conclusions

Soil erosion has substantial impact on natural and physical environment in North-eastern of Algeria semiarid zone. The present study proved that GIS and RS techniques are powerful tools for assessing waterborne erosion and for the estimation of soil loss in the Meskiana catchment. The adaptation of the empirical models of Wischmeier and Smith in the revised versions RUSLE model made possible to quantify the specific degradation due to the phenomenon. The process resulted from the combined effect of several natural and anthropogenic factors such as rainfall, soil texture, topography, land use, and human practices. The soil erosion susceptibility map was assessed by combining layers' maps of those factors. The GIS analysis has been carried out to estimate the annual soil loss on a pixel-by-pixel basis and the spatial distribution of the waterborne erosion area in the Meskiana catchment. The results proved the critical state of the soil in the catchment and how much human practices have deteriorated the natural environment in the study zone. We assessed the average loss at 61 t/ha/year with a total weight of 742,674 t/year for the entire basin. The losses vary from a minimum in the matorrals to a maximum value in rangelands. The land planted by cereal cultivation and seasonal crops are the most susceptible. Highest rates of eroded areas were recorded in the eastern and north-eastern part of the basin on marl outcrops. Whereas, the lowest rates

were recorded in the right bank of the basin where scrub of holm oak and trees covers the sandstone outcrops. These values not much different from those recorded in similar environments in NE Algeria. The comparison of mathematical methods with deterministic ones makes possible to identify the mineralogy and geochemistry of the soils most vulnerable to erosion. The adopted method can be applied in the entire Medjerda-Mellegue transboundary basin for the erosive potential estimation. It would help to take suitable erosion control measures in the severely affected areas; and could assists decision makers to implement mitigation measures in North East of Algeria.

Acknowledgements This work was overseen by the International Association of Water Resources in the Southern Mediterranean Basin-Tunisia and the Emerging Materials Research Unit, University of Ferhat Abbas, Setif, Algeria. The authors are indebted to the Laboratory of Applied Research in Engineering Geology, Geotechnics, Water Sciences, and Environment, Setif 1 University, Algeria. Acknowledgments to the General Directorate of Scientific Research and Technological Development (DGRSDT-MESRS) for the technical support. Tribute to the editor and reviewers for their valuable improvement on the manuscript.

Funding The authors declare and confirm that no exist any sources of funding (institutional, private, and corporate financial support) for the work reported in this paper.

Declarations

Conflict of interest On behalf of all authors, the corresponding author states that there is no conflict of interest. No participating authors have a financial or personal relationship with a third party whose interests could influence by the article's content.

References

- Aiello A, Adamo M, Canora F (2015) Remote sensing and GIS to assess soil erosion with RUSLE3D and USPED at river basin scale in southern Italy. *CATENA* 131:174–185
- Alexakis DD, Hadjimitsis DG, Agapiou A (2013) Integrated use of remote sensing, GIS and precipitation data for the assessment of soil erosion rate in the catchment area of "Yialias" in Cyprus. *Atmos Res* 131:108–124
- Anis Z, Wissem G, Riheb H, Biswajeet P, Essghaier GM (2019) Effects of clay properties in the landslides genesis in flysch massif: case study of Aïn Draham, North Western Tunisia. *J Afr Earth Sc* 151:146–152
- Arnoldus HMJ (1980) An approximation of the rainfall factor in the universal soil loss equation. *Approx Rainfall Factor Univ Soil Loss Eq*, 127–132.

- Benmarce K, Hadji R, Zahri F, Khanchoul K, Chouabi A, Zighmi K, Hamed Y (2021) Hydrochemical and geothermometry characterization for a geothermal system in semiarid dry climate: the case study of Hamma spring (north-east Algeria). *J Afr Earth Sci* 104285.
- Benselama O, Mazour M, Hasbaia M, Djoukbal O, Mokhtari S (2018) Prediction of water erosion sensitive areas in Mediterranean watershed, a case study of Wadi El Maleh in north-west of Algeria. *Environ Monit Assess* 190(12):1–15
- Bensoltane MA, Zeghadnia L, Hadji R (2021) Physicochemical characterization of drinking water quality of the communal water distribution network in Souk Ahras City/Algeria. *Civil Eng Res J* 12(02).
- Besser H, Mokadem N, Redhaouia B, Hadji R, Hamad A, Hamed Y (2018) Groundwater mixing and geochemical assessment of low-enthalpy resources in the geothermal field of southwestern Tunisia. *Euro-Mediterranean J Environ Integr* 3(1):16
- Besser H, Dhaouadi L, Hadji R, Hamed Y, Jemmali H (2021) Ecologic and economic perspectives for sustainable irrigated agriculture under arid climate conditions: an analysis based on environmental indicators for southern Tunisia. *J Afr Earth Sci*, 104134.
- Bouguerra, H, Bouanani A, Khanchoul K, Derdous O, Tachi SE (2017) Mapping erosion prone areas in the Bouhamdane watershed (Algeria) using the revised universal soil loss equation through GIS. *J Water Land Dev*
- Boulema S, Hadji R, Hamimed M (2021) Depositional environment of phosphorites in a semiarid climate region, case of El Kouif area (Algerian–Tunisian border). *Carbonates Evap* 36(3):1–15
- Brahmi S, Baali F, Hadji R, Brahmi S, Hamad A, Rahal O, Hamed Y (2021) Assessment of groundwater and soil pollution by leachate using electrical resistivity and induced polarization imaging survey, case of Tebessa municipal landfill NE Algeria Arabian. *J Geosci* 14(4):1–13
- Cassol EA, Silva TSD, Eltz FLF, Levien R (2018) Soil erodibility under natural rainfall conditions as the K factor of the universal soil loss equation and application of the nomograph for a subtropical Ultisol. *Revista Brasileira de Ciéncia do Solo* 42
- Dahoua L, Yakovitch SV, Hadji RH (2017a) GIS-based technic for roadside-slope stability assessment: an bivariate approach for A1 East-west highway, North Algeria. *Min Sci* 24
- Dahoua L, Yakovitch SV, Hadji R, Farid Z (2017b) Landslide susceptibility mapping using analytic hierarchy process method in BBA-Bouira Region, case study of east-west highway, NE Algeria. In: *Euro-mediterranean conference for environmental integration*. Springer, Cham, pp 1837–1840
- Dahoua L, Usychenko O, Savenko VY, Hadji R (2018) Mathematical approach for estimating the stability of geotextile-reinforced embankments during an earthquake. *Min Sci* 25
- Demdoum A, Hamed Y, Feki M, Hadji R, Djebbar M (2015) Multi-tracer investigation of groundwater in El Eulma Basin (Northwestern Algeria) North Africa. *Arab J Geosci* 8(5):3321–3333
- El Mekki A, Hadji R, Chemseddine F (2017) Use of slope failures inventory and climatic data for landslide susceptibility, vulnerability, and risk mapping in souk Ahras region. *Min Sci* 24
- Fredj M, Hafsaoui A, Riheb H, Boukarm R, Saadoun A (2020) Back-analysis study on slope instability in an open pit mine (Algeria). *Natsional'nyi Hirnychiy Universytet Naukovyi Visnyk* 2:24–29
- Ganasri BP, Ramesh H (2016) Assessment of soil erosion by RUSLE model using remote sensing and GIS-A case study of Nethravathi Basin. *Geosci Front* 7(6):953–961
- Gitas IZ, Douros K, Minakou C, Silleos GN, Karydas CG (2009) Multi-temporal soil erosion risk assessment in N. Chalkidiki using a modified USLE raster model. *EARSel proc* 8(1):40–52
- Hadji R, Limani Y, Baghem M, Demdoum A (2013) Geologic, topographic and climatic controls in landslide hazard assessment using GIS modeling: a case study of Souk Ahras region, NE Algeria. *Quatern Int* 302:224–237
- Hadji R, Limani Y, Demdoum A (2014a) Using multivariate approach and GIS applications to predict slope instability hazard case study of Machrouha municipality, NE Algeria. In: *2014a 1st international conference on information and communication technologies for disaster management (ICT-DM)*, pp 1–10. IEEE
- Hadji R, Limani Y, Boumazbeur AE, Demdoum A, Zighmi K, Zahri F, Chouabi A (2014b) Climate change and its influence on shrinkage–swelling clays susceptibility in a semi-arid zone: a case study of Souk Ahras municipality, NE-Algeria. *Desalin Water Treatment* 52(10–12):2057–2072
- Hadji R, Chouabi A, Gadri L, Raïs K, Hamed Y, Boumazbeur A (2016) Application of linear indexing model and GIS techniques for the slope movement susceptibility modeling in Bousselem upstream basin Northeast Algeria. *Arab J Geosci* 9(3):192
- Hadji R, Raïs K, Gadi L, Chouabi A, Hamed Y (2017) Slope failure characteristics and slope movement susceptibility assessment using GIS in a medium scale: a case study from Ouled Driss and Machrouha municipalities, Northeast Algeria. *Arab J Sci Eng* 42(1):281–300
- Hamad A, Hadji R, Bâali F, Houda B, Redhaouia B, Zighmi K, Hamed Y (2018a) Conceptual model for karstic aquifers by combined analysis of GIS, chemical, thermal, and isotopic tools in Tuniso-Algerian transboundary basin. *Arab J Geosci* 11(15):1–16
- Hamad A, Baali F, Hadji R, Zerrouki H, Besser H, Mokadem N, Hamed Y (2018b) Hydrogeochemical characterization of water mineralization in Tebessa-Kasserine karst system (Tuniso-Algerian Transboundary basin). *Euro-Mediterranean J Environ Integr* 3(1):7
- Hamad A, Hadji R, Boubaya D, Brahmi S, Baali F, Legrioui R, Hamed Y (2021a) Integrating gravity data for structural investigation of the Youkous-Tebessa and Fousana-Talah transboundary basins (North Africa). *Euro-Mediterranean J Environ Integr* 6(2):1–11
- Hamad A, Abdeslam I, Fehdi C, Badreddine S, Mokadem N, Legrioui R, Hamed Y (2021b) Vulnerability characterization for multi-carbonate aquifer systems in semiarid climate, case of Algerian–Tunisian transboundary basin. *Int J Energy Water Resour* 1–14

- Hamed Y, Ahmadi R, Hadji R, Mokadem N, Ben Dhia H, Ali W (2014) Groundwater evolution of the Continental Intercalaire aquifer of Southern Tunisia and a part of Southern Algeria: use of geochemical and isotopic indicators. *Desalin Water Treat* 52:10–12
- Hamed Y, Hadji R, Redhaouia B, Zighmi K, Bâali F, El Gayar A (2018) Climate impact on surface and groundwater in North Africa: a global synthesis of findings and recommendations. *Euro-Mediterranean J Environ Integr* 3(1):1–15
- Hamed Y, Hadji R, Ncibi K, Hamad A, Ben Sâad A, Melki A, Mustafa E (2021) Modelling of potential groundwater artificial recharge in the transboundary Algero-Tunisian Basin (Tebessa-Gafsa): the application of stable isotopes and hydroinformatics tools. *Irrigation Drain*
- Karaburun A (2010) Estimation of C factor for soil erosion modeling using NDVI in Buyukcekmece watershed. *Ozean J Appl Sci* 3(1):77–85
- Manchar N, Benabbas C, Hadji R, Bouaicha F, Grecu F (2018) Landslide susceptibility assessment in Constantine region (NE Algeria) by means of statistical models. *Stud Geotech Mech* 40(3)
- Merritt WS, Letcher RA, Jakeman AJ (2003) A review of erosion and sediment transport models. *Environ Model Softw* 18(8–9):761–799
- Mohammed S, Alsafadi K, Talukdar S, Kiwan S, Hennawi S, Alshihabi O, Harsanyie E (2020) Estimation of soil erosion risk in southern part of Syria by using RUSLE integrating geo informatics approach. *Remote Sens Appl Soc Environ* 20:100375
- Mokadem N, Demdoum A, Hamed Y, Bouri S, Hadji R, Boyce A, Laouar R, Saad A (2016) Hydrogeochemical and stable isotope data of groundwater of a multi-aquifer system: Northern Gafsa basin e Central Tunisia. *J Afr Earth Sc* 114:174–191
- Moore LD, Burch GJ (1985) Physical basis of the length-slope factor in the universal soil loss equation. *Soil Sci Soc Am J* 50:1294–1298
- Mouici R, Baali F, Hadji R, Boubaya D, Audra P, Fehdi CÉ, Arfib B (2017) Geophysical, geotechnical, and speleologic assessment for karst-sinkhole collapse genesis in Cheria plateau (NE Algeria). *Min Sci* 24:59–71
- Ncibi K, Char H, Hadji R, Baccari N, Sebei A, Khelifi F, Hamed Y (2020a) A GIS-based statistical model for assessing groundwater susceptibility index in shallow aquifer in Central Tunisia (Sidi Bouzid basin). *Arab J Geosci* 13(2):98
- Ncibi K, Hadji R, Hamdi M, Mokadem N, Abbes M, Khelifi F, Hamed Y (2020b) Application of the analytic hierarchy process to weight the criteria used to determine the Water Quality Index of groundwater in the northeastern basin of the Sidi Bouzid region, Central Tunisia. *Euro-Mediterranean J Environ Integr* 5:1–15
- Ncibi K, Hadji R, Hajji S, Besser H, Hajlaoui H, Hamad A, Hamed Y (2021) Spatial variation of groundwater vulnerability to nitrate pollution under excessive fertilization using index overlay method in central Tunisia (Sidi Bouzid basin). *Irrigation Drain*
- Nekkoub A, Baali F, Hadji R, Hamed Y (2020) The EPIK multi-attribute method for intrinsic vulnerability assessment of karstic aquifer under semi-arid climatic conditions, case of Cheria Plateau, NE Algeria. *Arab J Geosci* 13(15):1–15
- Nezhadafzali K, Shahrokhi MR, Bayatani F (2019) Assessment soil erosion using RUSLE model and identification the most effective factor in Dekhan watershed basin of southern Kerman. *J Natl Environ Hazards* 8(20):21–38
- Oldeman LR, Hakkeling RTA, Sombroek WG, Batjes N (1991) Global assessment of human-induced soil degradation. World map of the status of human-induced soil degradation
- Panditharathne DLD, Abeysingha NS, Nirmanee KGS, Mallawatantri A (2019) Application of revised universal soil loss equation (RUSLE) model to assess soil erosion in “Kalu Ganga” River Basin in Sri Lanka. *Appl Environ Soil Sci*
- Rais K, Kara M, Gadri L, Hadji R, Khochmen L (2017) Original Approach for the drilling process optimization in open cast mines; case study of Kef Essenoun open pit mine Northeast of Algeria. *Min Sci* 24
- Rango A, Arnoldus HMJ (1987) Aménagement des BV. *Cahiers techniques de la FAO*, 36
- Renard KG (1997) Predicting soil erosion by water: a guide to conservation planning with the Revised Universal Soil Loss Equation (RUSLE). United States Government Printing
- Rouabhia A, Djabri L, Hadji R, Baali F, Fahdi Ch, Hanni A (2012) Geochemical characterization of groundwater from shallow aquifer surrounding Fetzara Lake NE Algeria. *Arab J Geosci* 5(1):1–13
- Shin GJ (1999) The analysis of soil erosion analysis in watershed using GIS. Department of Civil Engineering, Gangwon National University, Gangwon-do, South Korea, Ph. D. dissertation
- Somasiri IS, Hewawasam T, Rambukkange MP (2021) Adaptation of the revised universal soil loss equation to map spatial distribution of soil erosion in tropical watersheds: a GIS/RS-based study of the Upper Mahaweli River. *Model Earth Syst Environ* 1–19
- Tamani F, Hadji R, Hamad A, Hamed Y (2019) Integrating remotely sensed and GIS data for the detailed geological mapping in semi-arid regions: Case of Youks les Bains Area, Tebessa Province, NE Algeria. *Geotech Geol Eng* 37(4):2903–2913
- Tamene L, Adimassu Z, Aynekulu E, Yaekob T (2017) Estimating landscape susceptibility to soil erosion using a GIS-based approach in Northern Ethiopia. *Int Soil Water Conserv Research* 5(3):221–230
- Teng H, Liang Z, Chen S, Liu Y, Rossel RAV, Chappell A, Shi Z (2018) Current and future assessments of soil erosion by water on the Tibetan Plateau based on RUSLE and CMIP5 climate models. *Sci Total Environ* 635:673–686
- Thapa P (2020) Spatial estimation of soil erosion using RUSLE modeling: a case study of Dolakha district. *Nepal Environ Syst Res* 9(1):1–10
- Viney NR, Sivapalan M (1999) A conceptual model of sediment transport: application to the Avon River Basin in Western Australia. *Hydrol Process* 13(5):727–743
- Williams JR, Berndt HD (1977) Sediment yield prediction based on watershed hydrology. *Trans ASAE* 20(6):1100–1104
- Wischmeier WH, Smith DD (1965) Predicting rainfall-erosion losses from cropland east of the Rocky Mountains: Guide for selection of practices for soil and water conservation (No. 282). Agricultural Research Service, US Department of Agriculture
- Wischmeier WH, Smith DD (1978) Predicting rainfall erosion losses: a guide to conservation planning (No. 537).

Department of Agriculture, Science and Education Administration

Xiao L, Yang X, Chen S, Cai H (2015) An assessment of erosivity distribution and its influence on the effectiveness of land use conversion for reducing soil erosion in Jiangxi, China. *CATENA* 125:50–60

Zeqiri RR, Riheb H, Karim Z, Younes G, Rania B, Aniss M (2019) Analysis of safety factor of security plates in the mine "Trepça" Stantërg. *Min Sci* 26:21

Publisher's Note Springer Nature remains neutral with regard to jurisdictional claims in published maps and institutional affiliations.